Synthesis and Systematic Evaluation of Dark Resonance Energy Transfer (DRET)-based Library and Its Application in Cell Imaging

Dongdong Su,[a],[b] Chai Lean Teoh,[b] Nam-Young Kang,[b] Xiaotong Yu,[a] Srikanta Sahu[b] and Young-Tae Chang*,[a],[b]

Abstract: In this paper, we report a new strategy for constructing large Stokes shift dye library. By coupling a dark donor with tunable high quantum yield BODIPY acceptors, a novel Dark Resonance Energy Transfer (DRET) based library, named **BNM**, has been synthesized. Upon excitation of the dark donor (**BDN**) at 490 nm, it was demonstrated that the absorbed energy was transferred to the acceptor (**BDM**) with high efficiency, which was tunable in a broad range from 557 nm to 716 nm, with high quantum yield of up to 0.8. It is noteworthy to mention that the majority of the non-radiative energy loss of donor was converted to the acceptor's fluorescence output with minimum leaks of donor emission. Fluorescence imaging tested in live cells showed that the **BNM** compounds are cell-permeable and can also be employed for live cell imaging. This is a new library which can be excited by dark donor to emit a tunable wide range of high fluorescence emission. Thus, the **BNM** library is well suited for high-throughput screening or multiplexing experiments in biological methods by using a single laser excitation source.

Introduction

Fluorescent labelling has been developed to be a powerful tool in many biochemical and medical diagnostics, which can provide visualization of organelles as well as real-time monitoring of biochemical processes.[1] In recent years, many approaches have been explored to develop fluorescent labeling technology, such as labeling of individual cells,[2] DNA sequencing labeling[3] and proteins labeling.[4] Among all these approaches, multicolor fluorescent labeling exhibits the advantages of time resolution, however, this approach has been hampered due to the limited availability of multicolor fluorescent molecules.

Up to now, antibody,[5] quantum dots[6] and organic dyes are the widely used signal reporters for specific labeling of targets, however, each of them has its drawbacks in multicolor fluorescent labeling technology. Different antibodies can provide specific labeling of cellular organelles in a multicolor format, but their relatively large size and poor cell permeability hindered their progress in practical biological applications.[7] Compared to other fluorophores, quantum dots show some advantages like having multiple colors and high photostability.[8] However, their cell toxicity and high consumption become their significant drawbacks.[9] Aside from antibody and quantum dots, small fluorescence molecules were also developed in the field of fluorescence labeling because of their sensitivity and easy visibility.[1b, 10] Till now, most of the multiplexing experiments have been achieved by using different structures of organic fluorophores for each color labeling.[11] However, using different organic dyes may suffer from photoinstability, pH and ionic sensitivity and may induce unpredictable interactions with various biopolymers during the experiments.[3c]

New fluorescence libraries based on DOFLA (diversity-oriented fluorescence library approach) reported by our group have led to the discovery of a series of novel sensors.[12] The DOFLA libraries which were constructed with the same fluorescence scaffold but with different building blocks can be used for multicolor labeling. The features of DOFLA libraries can potentially overcome some of the drawbacks caused by fluorophores with different structures.[13] Single fluorescent core structure can show tunable emission and even predictable photophysical properties.[14] However, for these published libraries, it was difficult to find one single wavelength excitation suitable for all these fluorophores with tunable emission. The dye at longer absorption wavelength cannot absorb enough energy to emit strong fluorescent intensities.[15]

With the involvement of Förster resonance energy transfer (FRET) approach, we can solve the above mentioned problems.[16] The FRET-based dyes are constructed with the same donor but different acceptors, which will allow us to obtain strong tunable emissions by exciting the same donor. Recently, our group reported a set of novel Dark Resonance Energy Transfer (DRET) dyes, **BNM**, which use low quantum yield donor (less than 1%) to emit a wide range of high fluorescence emission.[17] The results show that the absorbed energy can be transferred to the acceptor with a high energy transfer rate, before being quenched by non-radiative intramolecular rotations. Also, this new designed DRET-based dyes show unique photophysical characteristics, such as high ability of light harvesting without fluorescence leaking from the donor, tunable emission wavelength excited at a single wavelength excitation, large pseudo-Stokes shifts and emission shifts, as well as highly efficient energy transfer. Furthermore, this type of dyes shows good cell penetration, which makes them as good candidate for living cells imaging.[17] All of these great properties encourage us to develop one library of **BNM** compounds and further study the relationship between structures and photophysical properties and then we can design and develop new **BNM** dyes for practical applications.

[a] D. Su, X. Yu and Prof. Y. T. Chang
Department of Chemistry & MedChem Program of Life Sciences
Institute National University of Singapore, 117543, Singapore
Tel: (65) 6516-6774, Fax: (+65) 6779-1691
E-mail: chmcyt@nus.edu.sg

[b] Dr. C. L. Teoh, Dr. N. Y. Kang, Dr. S. Sahu and Prof. Y. T. Chang
Singapore Bioimaging Consortium, Agency for Science, Technology and Research (A*STAR), 138667, Singapore

Supporting information for this article is given via a link at the end of the document.((Please delete this text if not appropriate))

Results and Discussion

Synthesis and Spectroscopic Properties of BNM Library

The **BNM** library was synthesized as reported (Scheme 1).[17] The synthesis of 80 members of **BDM** was reported previously by our group.[18] Same donor and different acceptors were connected by cyanuric chloride, which contains features of good biocompatibility with various biological effects.[19] First, **BDN-1** was reacted with cyanuric chloride linker to obtain an intermediate **BDN-3**. After this key intermediate **BDN-3** was efficiently synthesized, the acceptors, **BDM**, were introduced by combinational synthesis method to make the final **BNM** library (Scheme S1 and Table S1). All compounds were purified by silica gel chromatography and characterized by HPLC/MS. The average purity was determined to be >90 % at 365 nm (Table S2).

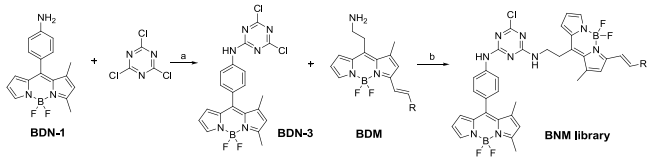

Scheme 1. Synthetic scheme of **BNM** library. Reagents and conditions: (a) DIEA, THF, 0 ºC, 1h; (b) DIEA, THF, rt, 2h. *R is from 80 commercial aldehydes.

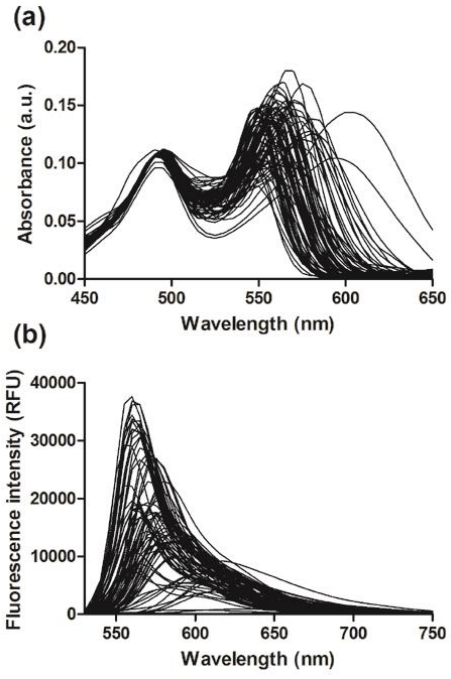

Figure 1. Spectroscopic properties of **BNM** library. Absorbance (a) and fluorescence spectra (b) of the **BNM** library (10 μM in EtOH, λ_{ex}= 490 nm).

The absorbance and fluorescence spectra of **BNM** library were measured with SpectraMax M2 spectrophotometer in EtOH. As shown in Figure 1a, all of the absorption spectra of **BNM** compounds displayed two featured peaks. The peak around 490 nm corresponded to the characteristic absorption signal of donor. And the other peak corresponded to the absorption signal of acceptors, which varied based on the broad chemical diversity of acceptor part. Compared with the unconjugated donor and acceptors, the shape of **BNM** absorption spectra did not show obvious change, which reveals that the electronic interactions between the donor and the acceptor are very weak.[20] The fluorescence spectra were obtained by exciting at the maximum absorption of **BDN-1** (490 nm), and their maximum emission varied in the range of 557 - 716 nm based on the emission of their corresponded acceptors (Figure 1b). The excitation and absorption spectra of **BNM** compounds also show good overlap, which confirms the intramolecular resonance energy transfer effect.[17a] It clearly showed that all members in **BNM** library can be excited at the same wavelength excitation but got various emission wavelengths. Also, it is worthy to mention there is no background influence from donor part due to the low quantum yield of donor, which made them ideal candidates for multicolor labeling. Benefited from the dark donor and high efficiency of energy transfer, different color and different quantum yield dyes can be generated in a smooth way.

Systematic Evaluation of Relationship between Structures and Photophysical Properties

To evaluate the relationship between quantum yield and maximum emission wavelength of the **BNM** compounds, we converted the data into a scatter plot of quantum yield for emission wavelength, as shown in Figure 2. An obvious trend can be observed: the quantum yield decreased with the red shift of emission. This result is reasonable, as the emission wavelength of the acceptors red shifted, the overlap between emission spectrum of the donor and absorption spectrum of the acceptor becomes less, even though the donor has rather small emission intensity. Comparing the statistical results and the structures of **BNM** acceptors, we found the relationships between the structures of **BNM** acceptors and the photophysical properties. As shown in Figure 2, we chose two representative types as example. The compounds in triangle show the highest quantum yield with emission wavelength at around 560 nm. Most of the compounds have similar features in their structures, which include the electro-donating group at the *ortho* position of the building block. As reported that the introduction of electro-donating group at the *ortho* positions can suppress non-radiative deactivation by restricting internal rotation of the phenyl ring, leading to relatively high quantum yield.[21] On the other hand, quite low quantum yields compounds also share similar structure features, containing the internal charge transfer (ICT) donor dialkylaminophenyl group in full conjugation with the BODIPY core (Table S3). As ICT process can quench the fluorescence of BODIPY core, and in addition, photoinduced electron transfer (PET) is known to be less significant in the longer wavelength region of the spectrum,[22] this explain the reasons for the low quantum yields of these dyes. It should be noted that based on the relationships between structures and photophysical data, we could predict and further design fluorophores with certain photophysical properties for particular application. For example, **BNM441** in square, which exhibits most of the desired photophysical properties for bioimaging and other biological

studies, such as long emission wavelength, high quantum yield and large pseudo-Stokes shifts. This may be because the structure of **BNM441** is more conjugated than those with dialkylaminophenyl substituent as building block, where the more conjugated structure can suppress the ICT process, which consequently shows longer emission wavelength and relatively high quantum yield.

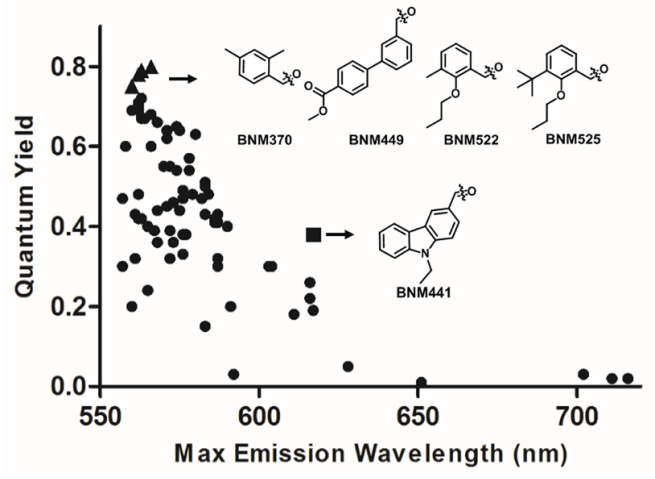

Figure 2. Relationship between structures and photophysical properties of **BNM** library.

As discussed above, the electronic character of the building block in the acceptors may crucially determine the photophysical properties of **BNM**. Up to now, Hammett substituent constant (σ) has already been used as a numerical value to quantitatively evaluate the electronic effects of a substituent.[23] To clarify the relationship between the structures and photophysical properties, we chose some compounds from the **BNM** library whose building blocks contain single *para*-position of the phenyl group substituents as examples. As shown in Table 1, Hammett substituent constant σ_p had a significant inverse correlation with the emission wavelength (Figure S1). The decrease in the Hammett substituent constant from highest ethyl (σ_p=−0.15) to lowest dimethylamine (σ_p=−0.83), caused bathochromic emission wavelength shifts from 562 to 716 nm (Table 1). Similar result was also discovered by the previous report.[14a] These trends further confirm the determined relationship between the electronic character of the building block and photophysical properties. In fact, the building blocks for most of the **BNM** compounds are complicated, containing two or three phenyl group substituents or conjugated structures, hence, the multiple electronic effects (*ortho*, *meta* and *para*) of substituents on the **BDM** acceptor may be responsible for the tunable emission wavelength of **BNM** library.

Application of BNM Compounds in Live Cell

Next, we examined the potential application of these new DRET compounds for fluorescence live cells imaging. All the **BNM** compounds were found to be well cell-permeable (data not shown). Among them, **BNM490** was observed to give the best-resolved images and its organelle localization in cells was further characterized (Figure 3). Co-staining with organelle tracker showed that **BNM490** co-localize with endoplasmic reticulum (ER) (Pearson's coefficients of 0.92). Taken together, the newly designed DRET-based **BNM** library being well penetrated in live cells renders it potentially useful for biological applications in living systems. In addition, we also demonstrate **BNM490**, as a new DRET-based ER sensor. It suggests that this new designed DRET-based **BNM** library is potentially useful for biological applications in living systems.

Table 1. Electronic effect of substituents on the relationship between structure and photophysical properties.

Compound	Substituent	Hammett constant [a]	λ_{abs}	λ_{em}
BNM2	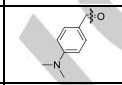	−0.83	494/594	716
BNM107	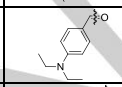	−0.72	494/595	711
BNM45	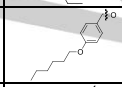	−0.34	494/559	576
BNM110	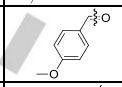	−0.27	494/557	573
BNM140	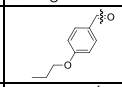	−0.25	494/559	573
BNM177	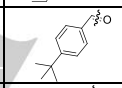	−0.20	494/553	562
BNM19	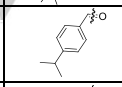	−0.15	494/552	562
BNM489	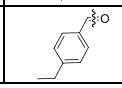	−0.15	494/551	562

[a] σ_p is the parameter for the Hammett constant of the *para*-position from reference.[23]

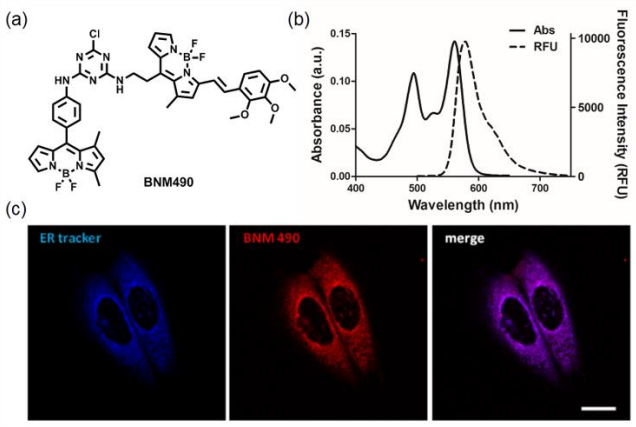

Figure 3. BNM490 stains endoplasmic reticulum of living cells. (a) Chemical structure of **BNM490**. (b) Absorbance and fluorescence spectra of **BNM490**. (c) Fluorescence images of CHO cells stained with 5 μM **BNM490** (red) (λ_{ex}=488 nm, λ_{em}=595 ±50 nm) and 1 μM of ER Tracker (blue) (λ_{ex}=405 nm, λ_{em}= 450 ±50 nm). Both images when merged show good correlation. The images were taken on a Nikon A1R$^+$si confocal microscope equipped with a 60× oil objective. Scale bar represents 20 μm.

Conclusions

By connecting dark donor and BODIPY acceptors, we have shown a new design and synthesis strategy of DRET-based library. This DRET strategy allows us to obtain a desired emission wavelength in biological experiments without considering the effective energy absorbed at the excitation wavelength. The **BNM** library is a novel BODIPY library with tunable emission wavelengths and high quantum yield using single excitation wavelength, which is particularly important for high-throughput screening or multiplexing technique. In addition, by analysing the relationship between building block structures and photophysical properties, fluorescent compounds with desired photophysical properties can be designed and synthesized by simple synthesis scheme. Also, cell imaging shows that **BNM** compounds were well cell-permeable and can be employed as well resolved fluorescence probe. With its unique properties, we believe that **BNM** compounds can be functionalized as excellent fluorescent probes for fluorescence labeling in bioimaging.

Experimental Section

Reagents and Solvents

The chemicals, including aldehydes and solvents, were purchased from Sigma Aldrich, Fluka, MERCK, Acros and Alfa Aesar. All the chemicals were directly used without further purification. Normal phase column chromatography purification was carried using MERCK silica Gel 60 (Particle size: 230-400 mesh, 0.040-0.063 mm).

Measurements and Analysis

HPLC-MS was taken on an Agilent-1200 with a DAD detector and a single quadrupole mass spectrometer (6130 series). The analytical method, unless indicated, is A: H_2O (0.1% HCOOH), B: CH_3CN (0.1% HCOOH), gradient from 10 to 90% B in 10 minutes; C18 (2) Luna column (4.6 ×50 mm^2, 3.5 µm particle size). Spectroscopic and quantum yield data were measured on a SpectraMax M2 spectrophotometer (Molecular Devices). Data analysis was performed using Graph Prism 5.0.

Quantum Yield Measurements

Quantum yields for all the fluorescent compounds were measured by dividing the integrated emission area of their fluorescent spectrum against the area of Rhodamine B in EtOH excited at 490 nm ($\Phi_{rho\text{-}B}$ = 0.7).[24] Quantum yields where then calculated using equation (1), where *F* represents the integrated emission area of fluorescent spectrum, η represents the refractive index of the solvent, and *Abs* represents absorbance at excitation wavelength selected for standards and samples. Emission was integrated from 530 nm to 750 nm.

$$\Phi_{flu}^{sample} = \Phi_{flu}^{reference}\left(\frac{F^{sample}}{F^{reference}}\right)\left(\frac{\eta^{sample}}{\eta^{reference}}\right)\left(\frac{Abs^{reference}}{Abs^{sample}}\right) \quad (1)$$

Cell Culture and Imaging Experiments

Chinese hamster ovary (CHO) cells were cultured in high-glucose (4500 mg/L) containing- Dulbecco's Modified Eagle's medium (DMEM) supplemented with 10 % fetal bovine serum, 100 U/ml penicillin and 100 µg/ml streptomycin. 24-36 h prior to imaging, cells were plated in clear bottom, 96-well plate or 35 mm glass bottom dish. **BNM** compounds were added to cultured cells to reach final concentration of 5-10 µM and incubated for 1 h at 37 ºC. Cells were washed with PBS buffer twice before imaging. To determine cell localization, ER-tracker Blue-White (1 µM) (Life Technologies) was added to **BNM**-stained CHO cells and further incubated for 15- 30 min at 37 ºC. Live cells images were acquired on an inverted Ti-E microscope (Nikon Instruments Inc), equipped with a customised Ex 480 nm/40, long-pass 510 nm filter for **BNM** fluorescence acquisition, as well as DAPI for Hoechst33342 fluorescence acquisition. Fluorescence imaging was also done on a Nikon $A1R^+si$ confocal microscope where mentioned. Images were analysed using NIS Elements 3.10 software.

Acknowledgements

This work was supported by intramural funding from A*STAR (Agency for Science, Technology and Research, Singapore) Biomedical Research Council and National Medical Research Council grant (NMRC/CBRG/0015/2012).

Keywords: Dark donor • Dark Resonance Energy Transfer (DRET) • Fluorescence • large Stokes shift • Cell imaging

[1] a) A. P. de Silva, H. Q. Gunaratne, T. Gunnlaugsson, A. J. Huxley, C. P. McCoy, J. T. Rademacher, T. E. Rice, *Chem. Rev.* **1997**, *97*, 1515-1566; b) L. D. Lavis, R. T. Raines, *ACS Chem. Boil.* **2008**, *3*, 142-155; c) M. S. Goncalves, *Chem. Rev.* **2009**, *109*, 190-212; d) H. Kobayashi, M. Ogawa, R. Alford, P. L. Choyke, Y. Urano, *Chem. Rev.* **2010**, *110*, 2620-2640.

[2] J. B. Delehanty, C. E. Bradburne, K. Susumu, K. Boeneman, B. C. Mei, D. Farrell, J. B. Blanco-Canosa, P. E. Dawson, H. Mattoussi, I. L. Medintz, *J. Am. Chem. Soc.* **2011**, *133*, 10482-10489.

[3] a) Z. Li, X. Bai, H. Ruparel, S. Kim, N. J. Turro, J. Ju, *Proc. Natl. Acad. Sci. U S A* **2003**, *100*, 414-419; b) M. L. Metzker, J. Lu, R. A. Gibbs, *Science* **1996**, *271*, 1420-1422; c) K. E. Sapsford, L. Berti, I. L. Medintz, *Angew. Chem. Int. Ed.* **2006**, *45*, 4562-4589.

[4] a) M. Hintersteiner, A. Enz, P. Frey, A. L. Jaton, W. Kinzy, R. Kneuer, U. Neumann, M. Rudin, M. Staufenbiel, M. Stoeckli, K. H. Wiederhold, H. U. Gremlich, *Nat. Biotech.* **2005**, *23*, 577-583; b) C. Ran, X. Xu, S. B. Raymond, B. J. Ferrara, K. Neal, B. J. Bacskai, Z. Medarova, A. Moore, *J. Am. Chem. Soc.* **2009**, *131*, 15257-15261; c) B. N. G. Giepmans, S. R. Adams, M. H. Ellisman, R. Y. Tsien, *Science* **2006**, *312*, 217-224.

[5] I. Morgado, K. Wieligmann, M. Bereza, R. Ronicke, K. Meinhardt, K. Annamalai, M. Baumann, J. Wacker, P. Hortschansky, M. Malesevic, C. Parthier, C. Mawrin, C. Schiene-Fischer, K. G. Reymann, M. T. Stubbs, J. Balbach, M. Gorlach, U. Horn, M. Fandrich, *Proc. Natl. Acad. Sci. U S A* **2012**, *109*, 12503-12508.

[6] A. Ekimov, *J. Lumin.* **1996**, *70*, 1-20.

[7] A. Miyawaki, A. Sawano, T. Kogure, *Nat. Cell Biol.* **2003**, *Suppl*, S1-7.

[8] J. B. Delehanty, C. E. Bradburne, K. Susumu, K. Boeneman, B. C. Mei, D. Farrell, J. B. Blanco-Canosa, P. E. Dawson, H. Mattoussi, I. L. Medintz, *J. Am. Chem. Soc.* **2011**, *133*, 10482-10489.

[9] J. Lovric, S. J. Cho, F. M. Winnik, D. Maysinger, *Chem. Biol.* **2005**, *12*, 1227-1234.

[10] B. N. Giepmans, S. R. Adams, M. H. Ellisman, R. Y. Tsien, *Science* **2006**, *312*, 217-224.

[11] a) J. H. Flanagan, Jr., C. V. Owens, S. E. Romero, E. Waddell, S. H. Kahn, R. P. Hammer, S. A. Soper, *Anal. Chem.* **1998**, *70*, 2676-2684; b) F. Samain, S. Ghosh, Y. N. Teo, E. T. Kool, *Angew. Chem. Int. Ed.* **2010**,

49, 7025-7029; c) V. Singh, S. Wang, E. T. Kool, *J. Am. Chem. Soc.* **2013**, *135*, 6184-6191.

[12] a) B. K. Wagner, H. A. Carrinski, Y. H. Ahn, Y. K. Kim, T. J. Gilbert, D. A. Fomina, S. L. Schreiber, Y. T. Chang, P. A. Clemons, *J. Am. Chem. Soc.* **2008**, *130*, 4208-4209; b) N. Y. Kang, H. H. Ha, S. W. Yun, Y. H. Yu, Y. T. Chang, *Chem. Soc. Rev.* **2011**, *40*, 3613-3626; c) M. Vendrell, D. T. Zhai, J. C. Er, Y. T. Chang, *Chem. Rev.* **2012**, *112*, 4391-4420.

[13] a) Y. H. Ahn, J. S. Lee, Y. T. Chang, *J. Am. Chem. Soc.* **2007**, *129*, 4510-4511; b) K. K. Ghosh, H. H. Ha, N. Y. Kang, Y. Chandran, Y. T. Chang, *Chem. Commun.* **2011**, *47*, 7488-7490; c) Q. A. Li, J. S. Lee, C. Ha, C. B. Park, G. Yang, W. B. Gan, Y. T. Chang, *Angew. Chem. Int. Ed.* **2004**, *43*, 6331-6335; d) G. R. Rosania, J. W. Lee, L. Ding, H. S. Yoon, Y. T. Chang, *J. Am. Chem. Soc.* **2003**, *125*, 1130-1131; e) S. L. Wang, Y. T. Chang, *J. Am. Chem. Soc.* **2006**, *128*, 10380-10381; f) S. L. Wang, Y. T. Chang, *Chem. Commun.* **2008**, 1173-1175.

[14] a) E. Kim, M. Koh, B. J. Lim, S. B. Park, *J. Am. Chem. Soc.* **2011**, *133*, 6642-6649; b) D. T. Zhai, S. C. Lee, M. Vendrell, L. P. Leong, Y. T. Chang, *Acs Comb. Sci.* **2012**, *14*, 81-84.

[15] G. S. Jiao, L. H. Thoresen, K. Burgess, *J. Am. Chem. Soc.* **2003**, *125*, 14668-14669.

[16] J. Fan, M. Hu, P. Zhan, X. Peng, *Chem. Soc. Rev.* **2013**, *42*, 29-43.

[17] a) D. Su, J. Oh, S. C. Lee, J. M. Lim, S. Sahu, X. Yu, D. Kim and Y. T. Chang, *Chem. Sci.* **2014**, 5, 4812–4818; b) D. Su, C. L. Teoh, S. Sahu, R. K. Das, Y. T. Chang, *Biomaterials* **2014**, *35*, 6078-6085.

[18] M. Vendrell, G. G. Krishna, K. K. Ghosh, D. T. Zhai, J. S. Lee, Q. Zhu, Y. H. Yau, S. G. Shochat, H. Kim, J. Chung, Y. T. Chang, *Chem. Commun.* **2011**, *47*, 8424-8426.

[19] a) C. H. Zhou, J. K. Min, Z. G. Liu, A. Young, H. Deshazer, T. Gao, Y. T. Chang, N. R. Kallenbach, *Bioorg. Med. Chem. Lett.* **2008**, *18*, 1308-1311; b) D. W. Jung, D. Williams, S. M. Khersonsky, T. W. Kang, N. Heidary, Y. T. Chang, S. J. Orlow, *Mol. Biosyst.* **2005**, *1*, 85-92; c) D. Williams, D. W. Jung, S. M. Khersonsky, N. Heidary, Y. T. Chang, S. J. Orlow, *Chem. Biol.* **2004**, *11*, 1251-1259; d) J. Min, Y. K. Kim, P. G. Cipriani, M. Kang, S. M. Khersonsky, D. P. Walsh, J. Y. Lee, S. Niessen, J. R. Yates, K. Gunsalus, F. Piano, Y. T. Chang, *Nat. Chem. Biol.* **2007**, *3*, 55-59.

[20] W. Y. Lin, L. Yuan, Z. M. Cao, Y. M. Feng, J. Z. Song, *Angew. Chem. Int. Ed.* **2010**, *49*, 375-379.

[21] a) H. Sunahara, Y. Urano, H. Kojima, T. Nagano, *J. Am. Chem. Soc.* **2007**, *129*, 5597-5604; b) K. Yamada, T. Toyota, K. Takakura, M. Ishimaru, T. Sugawara, *New. J. Chem.* **2001**, *25*, 667-669.

[22] a) T. Kobayashi, Y. Urano, M. Kamiya, T. Ueno, H. Kojima, T. Nagano, *J. Am. Chem. Soc.* **2007**, *129*, 6696-6697; b) Y. Fujikawa, Y. Urano, T. Komatsu, K. Hanaoka, H. Kojima, T. Terai, H. Inoue, T. Nagano, *J. Am. Chem. Soc.* **2008**, *130*, 14533-14543.

[23] C. Hansch, A. Leo, R. W. Taft, *Chem. Rev.* **1991**, *91*, 165-195.

[24] F. L. Arbeloa, P. R. Ojeda, I. L. Arbeloa, *J Lumin* **1989**, *44*, 105-112.

Entry for the Table of Contents

FULL PAPER

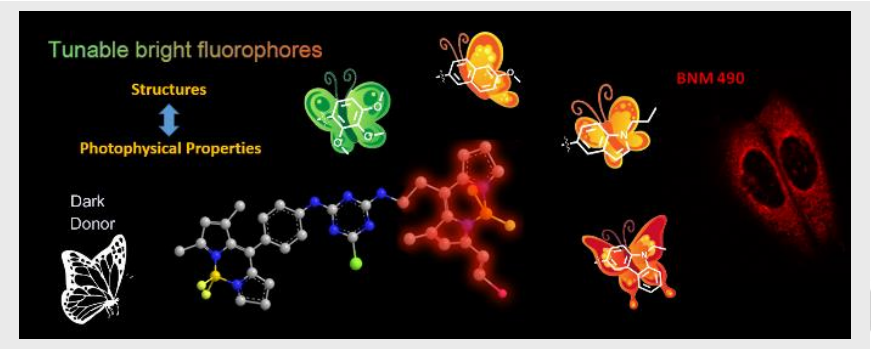

*Dongdong Su, Chai Lean Teoh, Nam-Young Kang, Xiaotong Yu, Srikanta Sahu and Young-Tae Chang**

Page No. – Page No.

Synthesis and Systematic Evaluation of Dark Resonance Energy Transfer (DRET)-based Library and Its Application in Cell Imaging

Dark Resonance Energy Transfer (DRET) strategy was reported for constructing large Stokes shift dye library. By coupling a dark donor with tunable high quantum yield BODIPY acceptors, a DRET-based library, named **BNM**, has been synthesized. Upon excitation of the dark donor, it was demonstrated that the absorbed energy was transferred to the acceptor with high efficiency. This is a new library which can be excited by dark donor to emit a tunable wide range of high fluorescence emission.

List of Contents

List of contents:

1. Table S1. Aldehyde building blocks for **BNM** library.

2. Table S2. Spectroscopic properties and purity table for **BNM** library.

3. Table S3. The summary of **BNM** compounds with low quantum yield.

4. Figure S1. Relationships between Hammett constant and maximum emission wavelength for the selected **BNM** compounds.

Table S1. Aldehyde building blocks for **BNM** library.

		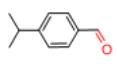	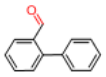	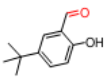	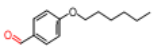
1	2	19	40	43	45
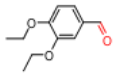	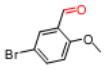			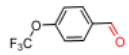	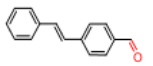
53	54	62	63	68	69
	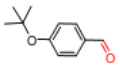		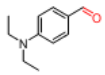	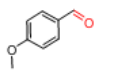	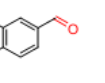
70	75	78	107	110	132
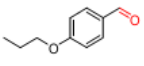	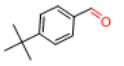	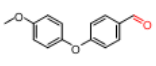	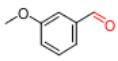	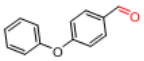	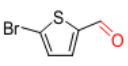
140	177	178	186	101	100
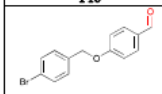	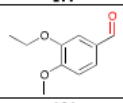	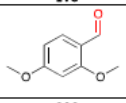	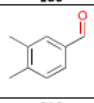	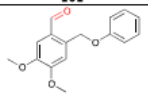	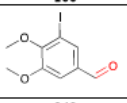
52	164	206	216	223	242
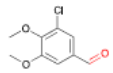	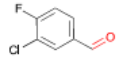	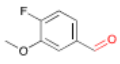	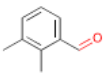	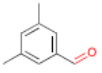	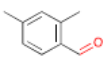
294	296	329	349	361	370
	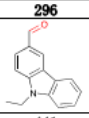	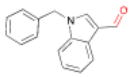	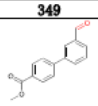		
375	441	446	449	455	456
468	472	474	483	486	487
489	490	491	495	498	505
506	507	510	511	513	515
516	517	518	519	520	522
524	525	526	527	528	529
530	531	532	533	143	198
397	401				

Table S2. Spectroscopic properties and purity table for **BNM** library: absorbance maximum (λ_{abs}), fluorescent emission maximum (λ_{em}), extinction coefficient and quantum yield.

Code	mass (calc)	m/z (exp)	λ_{abs} (nm)	λ_{em} (nm)	ε ($M^{-1}cm^{-1}$)[a]	Φ[b]	Purity (%)
BNM-1	863.3	862.2	494/555	572	61169	0.32	90
BNM-2	816.3	817.3	494/594	716	57652	0.02	91
BNM-19	815.3	814.3	494/552	562	79522	0.42	91
BNM-40	849.3	848.2	494/554	565	55311	0.40	86
BNM-43	845.3	846.3	494/561	576	49680	0.33	92
BNM-45	873.4	874.4	494/559	576	65109	0.38	90
BNM-53	861.3	862.3	494/561	586	61765	0.42	99
BNM-54	881.2	881.0	494/554	568	74195	0.44	82
BNM-62	833.3	832.2	494/561	582	61765	0.47	93
BNM-63	847.3	846.2	494/561	586	91254	0.41	90
BNM-68	857.3	858.3	494/548	557	56300	0.47	99
BNM-69	875.3	876.4	494/569	583	103329	0.51	96
BNM-70	883.3	882.2	494/576	617	66298	0.19	92
BNM-75	845.3	844.3	494/555	572	58136	0.39	88
BNM-78	861.3	860.3	494/583	651	69380	0.01	96
BNM-107	844.3	843.2	494/595	711	81103	0.02	90
BNM-110	803.3	802.2	494/557	573	67470	0.46	90
BNM-132	819.3	818.2	494/561	583	81692	0.15	99
BNM-140	831.3	830.3	494/559	573	68094	0.46	90
BNM-177	829.3	810.3	494/553	562	62674	0.42	86
BNM-178	895.3	894.3	494/557	571	77863	0.45	88
BNM-186	803.3	802.2	494/550	561	53540	0.43	89
BNM-101	865.3	864.3	494/555	568	86069	0.36	86
BNM-100	857.1	858.1	494/565	576	78504	0.47	88
BNM-52	957.2	956.2	494/557	572	80610	0.55	89
BNM-164	847.3	848.3	494/560	583	83940	0.43	97

BNM-206	833.3	834.3	494/565	587	78472	0.43	90
BNM-216	801.3	802.3	494/552	563	85037	0.67	99
BNM-223	939.3	938.3	494/572	628	85063	0.05	91
BNM-242	959.2	958.2	494/554	566	87888	0.68	98
BNM-294	867.3	868.2	494/553	564	83537	0.67	99
BNM-296	825.2	826.2	494/547	558	64547	0.60	95
BNM-329	821.3	822.3	494/549	560	84972	0.69	99
BNM-349	801.3	802.3	494/547	562	72602	0.70	86
BNM-361	801.3	802.3	494/549	560	79003	0.69	97
BNM-370	801.3	802.3	494/553	566	68095	0.80	99
BNM-375	812.3	812.3	494/576	616	70913	0.22	94
BNM-441	890.3	891.4	494/577	617	94473	0.38	97
BNM-446	902.3	883.3	494/582	616	78151	0.26	90
BNM-449	907.3	888.3	494/549	560	85900	0.75	97
BNM-455	812.3	813.3	494/558	565	55643	0.24	89
BNM-456	812.3	813.3	494/571	557	56087	0.30	86
BNM-468	901.3	882.3	494/576	560	62974	0.20	91
BNM-472	828.3	813.3	494/549	561	57222	0.32	95
BNM-474	801.3	802.3	494/549	562	76570	0.69	99
BNM-483	909.3	890.3	494/557	574	76687	0.54	99
BNM-486	831.3	832.3	494/559	575	74731	0.44	85
BNM-487	911.2	894.2	494/562	578	80133	0.54	91
BNM-489	801.3	802.3	494/551	562	68562	0.48	98
BNM-490	863.3	864.3	494/554	570	78471	0.55	86
BNM-491	812.3	813.3	494/565	587	83859	0.30	93
BNM-495	853.3	854.3	494/563	580	98822	0.63	97
BNM-498	858.3	859.4	494/572	702	81732	0.03	89
BNM-505	903.3	882.3	494/559	592	83608	0.03	91

BNM-506	859.3	860.4	494/557	571	78855	0.62	97
BNM-507	817.3	818.3	494/550	562	82019	0.71	95
BNM-510	817.3	818.3	494/559	576	79322	0.49	86
BNM-511	959.2	958.2	494/557	574	77110	0.65	93
BNM-513	826.3	827.3	494/572	603	86842	0.30	97
BNM-515	831.3	832.3	494/553	566	61765	0.60	99
BNM-516	826.3	827.3	494/565	587	61765	0.32	90
BNM-517	919.4	918.4	494/558	577	85761	0.38	97
BNM-518	885.4	888.4	494/558	571	78928	0.64	99
BNM-519	889.4	890.3	494/561	587	84056	0.41	93
BNM-520	889.4	890.4	494/551	563	83016	0.72	99
BNM-522	845.3	846.3	494/550	562	84907	0.78	97
BNM-524	891.3	892.3	494/559	573	90672	0.36	86
BNM-525	887.4	888.4	494/550	563	80831	0.79	98
BNM-526	845.3	846.3	494/560	578	84565	0.57	99
BNM-527	987.2	986.2	494/558	575	78302	0.64	96
BNM-528	875.3	876.3	494/561	584	93895	0.48	99
BNM-529	854.3	855.3	494/572	604	82420	0.30	96
BNM-530	854.3	855.3	494/574	611	76304	0.18	97
BNM-531	859.3	860.3	494/554	568	86484	0.66	99
BNM-532	854.3	855.3	494/566	590	90153	0.40	97
BNM-533	861.3	862.3	494/562	583	86692	0.50	93
BNM-143	787.3	788.3	494/549	563	45834	0.42	89
BNM-198	803.3	804.3	494/554	567	51689	0.39	89
BNM-397	833.3	834.3	494/562	591	64421	0.20	90
BNM-401	891.3	892.3	494/562	579	66165	0.48	96

[a]The maximal absorption of the **BDM** part; [b]Fluorescence quantum yields were determined using rhodamine B (Φ=0.7 in EtOH) as a standard. All absorbance and fluorescence excitation and emission

data were recorded by SpectraMax M2, Molecular Devices, fluorescent plate reader (10 μM compounds in EtOH (100 μL) for λ_{abs}, 10 μM compounds in EtOH (100 μL) for λ_{em} in 96-well polypropylene plates. Mass was calculated as (M+), and found in ESI-MS (M-F), or found mass (M+H) in the positive mode scan, or found mass (M-H) in the negative mode scan; Purity data was calculated on the basis of the integration in HPLC trace at 365 nm.

Table S3. The summary of **BNM** compounds with low quantum yield.

Compound code	Substituent	λ_{abs}	λ_{em}	Φ
BNM2	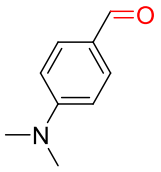	494/594	716	0.02
BNM78	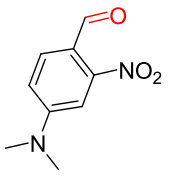	494/583	651	0.01
BNM107	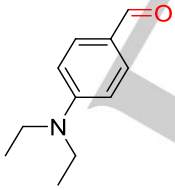	494/595	711	0.02
BNM498	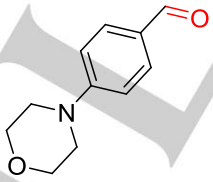	494/572	702	0.03
BNM505	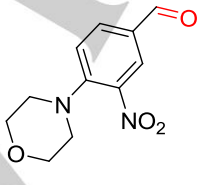	494/559	592	0.03

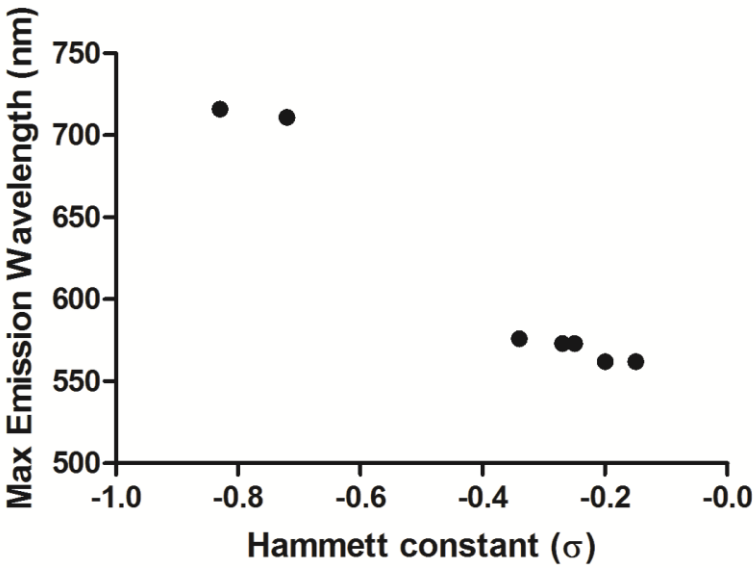

Figure S1. Relationship between Hammett constant and maximum emission wavelength for selected **BNM** compounds.